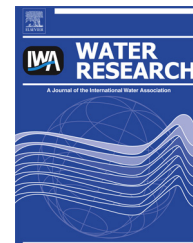




ELSEVIER

Available online at www.sciencedirect.com

SciVerse ScienceDirect

journal homepage: www.elsevier.com/locate/watres

Tight ceramic UF membrane as RO pre-treatment: The role of electrostatic interactions on phosphate rejection

Ran Shang^{a,*}, Arne R.D. Verliefde^{a,b}, Jingyi Hu^a, Zheyi Zeng^a, Jie Lu^a, Antoine J.B. Kemperman^c, Huiping Deng^d, Kitty Nijmeijer^c, Sebastiaan G.J. Heijman^a, Luuk C. Rietveld^a

^a Department of Sanitary Engineering, Faculty of Civil Engineering and Geosciences, Delft University of Technology, P.O. Box 5048, 2600 GA Delft, The Netherlands

^b Particle and Interfacial Technology Group, Faculty of Bioscience Engineering, Ghent University, Coupure Links 653, 9000 Ghent, Belgium

^c Membrane Science and Technology, MESA+ Institute for Nanotechnology, Faculty of Science and Technology, University of Twente, P.O. Box 217, NL-7500 AE Enschede, The Netherlands

^d Key Laboratory of Yangtze River Water Environment, Ministry of Education, Tongji University, 200092 Shanghai, China

ARTICLE INFO

Article history:

Received 24 July 2013
Received in revised form
28 September 2013
Accepted 2 October 2013
Available online xxx

Keywords:

Electrostatic repulsion
Donnan exclusion
Tight ultrafiltration
Phosphate rejection
Phosphate limitation
Biofouling
Ceramic membrane

ABSTRACT

Phosphate limitation has been reported as an effective approach to inhibit biofouling in reverse osmosis (RO) systems for water purification. The rejection of dissolved phosphate by negatively charged TiO₂ tight ultrafiltration (UF) membranes (1 kDa and 3 kDa) was observed. These membranes can potentially be adopted as an effective process for RO pre-treatment in order to constrain biofouling by phosphate limitation. This paper focuses on electrostatic interactions during tight UF filtration. Despite the larger pore size, the 3 kDa ceramic membrane exhibited greater phosphate rejection than the 1 kDa membrane, because the 3 kDa membrane has a greater negative surface charge and thus greater electrostatic repulsion against phosphate. The increase of pH from 6 to 8.5 led to a substantial increase in phosphate rejection by both membranes due to increased electrostatic repulsion. At pH 8.5, the maximum phosphate rejections achieved by the 1 kDa and 3 kDa membrane were 75% and 86%, respectively. A Debye ratio (ratio of the Debye length to the pore radius) is introduced in order to evaluate double layer overlapping in tight UF membranes. Threshold Debye ratios were determined as 2 and 1 for the 1 kDa and 3 kDa membranes, respectively. A Debye ratio below the threshold Debye ratio leads to dramatically decreased phosphate rejection by tight UF membranes. The phosphate rejection by the tight UF, in combination with chemical phosphate removal by coagulation, might accomplish phosphate-limited conditions for biological growth and thus prevent biofouling in the RO systems.

© 2013 Elsevier Ltd. All rights reserved.

* Corresponding author. Tel.: +31 15 2783539.

E-mail addresses: R.Shang@tudelft.nl, r.shang@outlook.com (R. Shang).

1. Introduction

Biofouling severely inhibits the wide application of reverse osmosis (RO) membranes in wastewater reclamation where nutrient concentrations are high in the secondary treated effluent (Shang et al., 2011; van Agtmaal et al., 2007). Phosphate (P) concentration is identified as a key factor in biofouling development. In drinking water distribution networks, microbial growth was notably enhanced by an increase of merely $1 \mu\text{g P L}^{-1}$ (Miettinen et al., 1997; Sathasivan et al., 1997). Recently, the concept of biofouling control in RO systems by P limitation was proposed (Jacobson et al., 2009; Vrouwenvelder et al., 2010). In the RO systems, a low P concentration of about $0.3 \mu\text{g L}^{-1}$ can alleviate the increase of trans-membrane pressure and prohibit accumulation of biomass in an RO feed-spacer, even when the feed matrix contains a high concentration of dissolved organic matter (Vrouwenvelder et al., 2010). On the other hand, calcium phosphate has been found as the key scalant in RO membranes during effluent water treatment for reuse, limiting the water recovery of the RO systems (Bartels et al., 2005; Greenberg et al., 2005). In addition, harsh chemical cleaning is not suitable for controlling biofouling in polymeric RO membranes where the skin layer is sensitive to chlorination and oxidants (Ang et al., 2006).

As a result, intense pre-treatment is applied to alleviate the biofouling and scaling in RO membranes during wastewater reclamation. Current filtration-based pre-treatment processes such as microfiltration, ultrafiltration, sand filtration, and granular activated carbon filters cannot adequately prevent biofouling due to their poor removal of nutrients from feed water (Herzberg et al., 2010; Schneider et al., 2005; Vrouwenvelder et al., 2010). Coagulation, as a conventional RO pre-treatment, is able to reduce the P concentration to $6\text{--}120 \mu\text{g L}^{-1}$ (Jacobson et al., 2009), which is not enough to restrict biofilm growth. Therefore, technologies with enhanced P removal are needed to inhibit the biofilm growth (Vrouwenvelder et al., 2010) as well as provide scaling control in membrane elements. Proposing effective pre-treatment methods to remove phosphate in the feed water is crucial for the control of biofouling in an RO membrane during wastewater reclamation.

A tight ceramic ultrafiltration membrane with molecular weight cut-off (MWCO) between 1 and 3 kDa can potentially be used as a novel method for RO pre-treatment. On one hand, more robust backwashing and harsh chemical cleaning can be applied to the tight ceramic UF membrane to control membrane fouling (Boley et al., 2010; Kim et al., 2008). On the other hand, rejection of charged solutes, such as phosphate, by a charged tight ceramic membrane can hypothetically be achieved due to electrostatic exclusion from a charged membrane.

Previous studies revealed that negatively charged NF (or negatively charged loose NF) membranes can obtain a higher rejection of charged organic acids (Bellona and Drewes, 2005) and ionized pharmaceuticals (Nghiem et al., 2006; Verliefde et al., 2008) than could be expected purely by steric exclusion. In addition, the electrostatic interactions also play a role in ionic rejection by tight polymeric UF or tight ceramic UF

membranes. A tight polysulfone UF membrane with an MWCO of 8 kDa was reported to be capable of rejecting anionic arsenate (Brandhuber and Amy, 1998; 2001). The studies on gamma alumina nanofiltration membranes, which are positively charged at pH 7, showed that the rejection of ionic species is dependent on the pH of the solutions and the results can be interpreted by Donnan exclusion and formation of an electrical double layer in the membrane pores (Alami-Younssi et al., 1995; Schaep et al., 1999). Labbez et al. (2003) explained that the greater ion rejection due to electrostatic repulsion may result from a stronger overlapping of the electrical double layers in pores. Unlike a polymeric membrane, the streaming potential (also called filtration potential) through the thick support layer of a ceramic NF membrane is not negligible, although its active layer plays a major role, as reported by Fievet et al. (2005). Moreover, dielectric exclusion plays an important role in ion rejection by NF membranes (Bandini and Vezzani, 2003; Déon et al., 2009; Szymczyk and Fievet, 2005), which is determined by the difference between the dielectric constant of the aqueous solution in the pores and the dielectric constant of the membrane material (Bandini and Vezzani, 2003). The dielectric exclusion can be stronger from pores with a closed geometry than from pores with a relatively open geometry (Yaroshchuk, 2000). Performances and mechanisms of P rejection by tight ceramic UF membranes, however, have not yet been investigated, while their potential benefits may be significant.

The aim of this study was to investigate the role of electrostatic interactions on phosphate rejection by tight ceramic UF membranes. The impact of solution chemistry (pH and ionic strength of the feed solution) on phosphate rejection was studied. Membrane surface charge was measured to elucidate the role of electrostatic repulsion on phosphate rejection. The Debye ratio, a parameter dependent on both ionic strength and membrane pore size, was used to explicate the essential conditions to achieve phosphate rejection by UF membranes. The effect of the physical parameters of the filtration process, such as permeate flux and cross-flow rate, were also delineated. Additionally, the possibility was discussed, that the phosphate adsorption on the ceramic membrane surface may be capable of changing the membrane surface charge (and thus zeta potential).

2. Materials and methods

2.1. Membrane and characterizations

2.1.1. Tight ceramic UF membranes

Two commercially available TiO_2 tight UF membranes (TAMI Industry, France) with MWCOs of 1 and 3 kDa were used in this study. The membranes have seven channels and a tubular configuration with dimensions of 10 mm in diameter and 250 mm in length. The effective filtration area of each membrane is 0.013 m^2 . The membrane is operated in the inside-out mode during filtration experiments. Membrane samples in the flat disc configuration were used for zeta potential measurement and EDX (energy dispersive x-ray) analysis. The flat disc membrane and the tubular membrane of the same MWCO

were fabricated by the same manufacturer following the identical recipe and procedures. Therefore, the characterizations on flat disc membranes are representative of the tubular membranes. More details of the membranes are shown in Supplementary Data, Table S1.

2.1.2. Zeta potential measurement

The zeta potential of the tight ceramic UF membranes was determined by the streaming potential method using an electrokinetic analyzer (SurPASS, Anton Paar, Graz, Austria) with an adjustable gap cell. It was measured in tangential mode and the charge was measured at the membrane surface. The zeta potential was automatically determined by the instrument using the Helmholtz–Smoluchowski equation (Christoforou et al., 1985). The measured values by this method are likely lower than the true values due to the ignored conductivity of the membrane material (Fievet et al., 2004, 2003; Yaroshchuk and Ribitsch, 2002). The zeta potential values obtained were the apparent values for qualitative comparison between different membranes in this study. Two types of electrolytes (Table 1) were used as background solutions during the zeta potential measurements. Besides the zeta potential measurement by NaCl electrolyte (electrolyte No. 1 in Table 1), an electrolyte with additional P (No. 2 in Table 1) was used to examine the effect of low concentrations of phosphate (i.e. potential adsorption of P on the membrane surface) on the zeta potential of both membranes. Each electrolyte was used to flush the cell thoroughly prior to the measurement. The pH of the electrolyte solutions, ranging from 6 to 9, was automatically adjusted with 0.1 mol L⁻¹ NaOH. All measurements were performed at room temperature (25 °C), which was monitored by the temperature probe of the instrument.

2.2. Experimental setup and filtration protocol

Phosphate rejection experiments were carried out with a bench-scale cross-flow filtration system (Supplementary Data, Figure S1). The filtration was conducted using a gear pump with feed water volume of 50 L. Both permeate and concentrate were recycled back into the feed tank. Water temperature was controlled at 20 ± 1 °C using a temperature controller. All filtration experiments were carried out at a constant cross-flow velocity and permeate flux. The flow was adjusted by a needle valve which was installed in the concentrate recirculation tube.

In the membrane filtration experiments, permeate samples were collected after 3 h of stabilization of the membrane filtration system. The permeate samples were taken at 1-hour intervals during filtration and the feed water samples were taken at the first hour and the last hour during filtration. Each

filtration experiment was carried out in duplicate with two membranes.

In addition to the membrane filtration experiments, static adsorption of phosphate was carried out using a flat disc tight ceramic UF membrane. Adsorption of phosphate by the tight ceramic UF membrane was determined using element measurements with an energy dispersive x-ray (EDX) analyzer (Ametek EDAX^{TSL}) (Luo et al., 2010). Prior to the EDX analysis, flat disc membrane specimens of the size 10 mm × 10 mm were submerged in three different types of solutions (Table 2). The immersed samples were placed in an incubator and stirred at 80 rpm at 20 °C for 4 h. After the adsorption, each membrane sample was carefully and briefly rinsed with ultrapure water and dried at 40 °C for 12 h.

2.3. Analytical methods

P concentrations in the feed water and permeate were measured using the Phosphate Cell Test (No. 1.14543.0001) with NOVA 60 Spectroquant[®] Merck following the method of ortho-phosphate measurement. The measuring range was 0.05–5.00 mg P L⁻¹. The standard deviation from 36 replications of this method was 0.024 mg P L⁻¹.

2.4. Theoretical analysis

When a membrane with a fixed surface charge is placed in an electrolyte, an electrical double layer forms at the membrane's surface and on the walls of the pores. The electrical potential in the membrane's pores and on the surface determines the salt rejection by the membrane. In the pores of the membrane, the potential decreases from the wall potential roughly linearly in the Stern layer, and then descends exponentially through the diffuse layer because of the gradual change of counter-ion concentration over the distance from the wall (Hunter, 1981). The Debye ratio, λ , defined as the ratio of the Debye length (κ^{-1}) to the pore radius, affects the potential distribution in the membrane's pores (Gross and Osterle, 1968).

The thickness of this electrical double layer can be characterized by the Debye length (κ^{-1}), defined by:

$$\kappa^{-1} = \left(\frac{\epsilon_0 \cdot \epsilon_r \cdot K_B \cdot T}{2000 \cdot N_A \cdot e^2 \cdot I} \right)^{\frac{1}{2}} \quad (1)$$

where, ϵ_0 is vacuum permittivity (8.85 × 10⁻¹² C V⁻¹ m⁻¹); ϵ_r is relative permittivity of the background solution (80 for water at 20 °C); K_B is the Boltzmann constant (1.38 × 10⁻²³ J K⁻¹); T is absolute temperature (K); N_A is the Avogadro number (6.0 × 10²³ mol⁻¹); e is the elementary charge (1.6 × 10⁻¹⁹ C); I is ionic strength (mol L⁻¹) (Hunter, 1981).

Table 1 – Background solutions for zeta potential measurements.

No.	NaCl, mmol L ⁻¹	NaH ₂ PO ₄ , mg P L ⁻¹	IS, mmol L ⁻¹
1	4.5	0	4.5
2	4.5	1.0	4.5

Table 2 – Solute chemistry of electrolytes for membrane rinsing prior to EDX analysis.

No.	NaCl, mmol L ⁻¹	NaH ₂ PO ₄ , mg P L ⁻¹
1 (DI water)	0	0
2	0	1.0
3	4.5	1.0

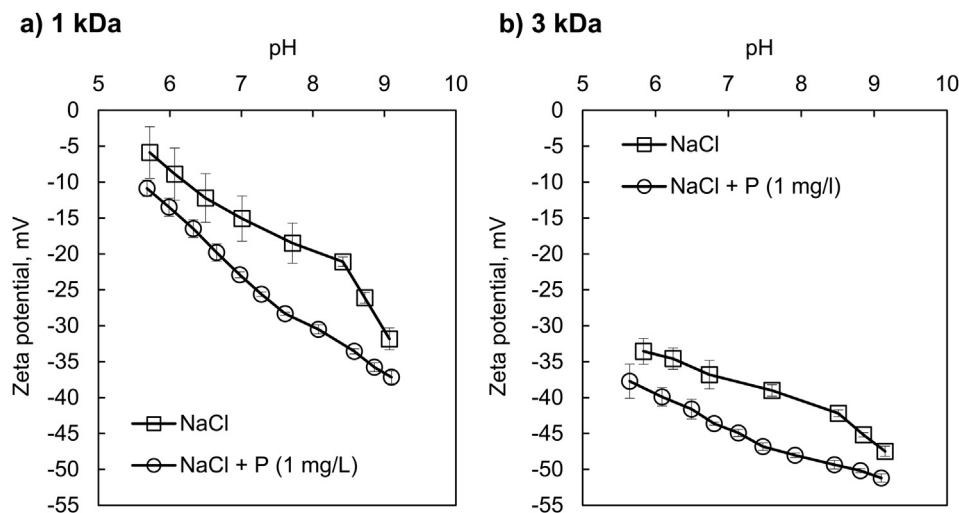


Fig. 1 – Surface zeta potential of a) 1 kDa and b) 3 kDa ceramic membrane in various electrolytes. Solute chemistry of electrolytes is shown in [Table 1](#).

The mean pore radius of the tight UF membranes can be calculated based on the MWCO using the Ferry–Faxen equation (Ferry, 1936):

$$(1 - R) = \left(1 - \frac{r_h}{r_p}\right)^2 \cdot \left(1 - 0.104 \frac{r_h}{r_p} - 5.21 \left(\frac{r_h}{r_p}\right)^2 + 4.19 \left(\frac{r_h}{r_p}\right)^3 + 4.18 \left(\frac{r_h}{r_p}\right)^4 - 3.04 \left(\frac{r_h}{r_p}\right)^5\right) \quad (2)$$

where, R is the dextran rejection; r_p is the pore radius of the membrane; r_h is the hydrodynamic radius of dextran. The r_h (in nm) can be converted from mean MW (in kDa) of the dextran by Eq. (3) (Dubin, 1988):

$$r_h = 0.845 \cdot \text{MW}^{0.498} \quad (3)$$

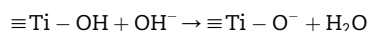
By combining Eqs. (2) and (3) and applying 90% retention of a dextran with molecular weight equal to MWCO (in kDa), the membrane pore size can be calculated by:

$$r_p = 2.10 \cdot r_h = 1.77 \cdot \text{MWCO}^{0.498} \quad (4)$$

3. Results and discussion

3.1. Membrane surface charge

The surface charge of both membranes increased as a function of pH within the range of 6–9 (Fig. 1), as the TiO_2 is amphoteric and the following reaction takes place (Larbot et al., 1988; Petersson et al., 2009):



As shown in Fig. 1, the isoelectric point (IEP) of both 1 kDa and 3 kDa membranes is expected to have a pH value lower than 6. This is consistent with previous studies which show that the IEP of TiO_2 -based ceramic membranes is in the pH range of 3.5–6.5 using the streaming potential method

(Chevereau et al., 2010; Huisman et al., 1998; Moritz et al., 2001; Parks, 1965; Tsuru et al., 2001).

The 3 kDa ceramic membrane consistently showed a higher negative charge than the 1 kDa ceramic membrane in the pH range investigated. This might be attributed to the different sintering processes in order to produce ceramic membranes of different MWCO, which likely alters the IEP value and surface charge (Kosmulski, 2003).

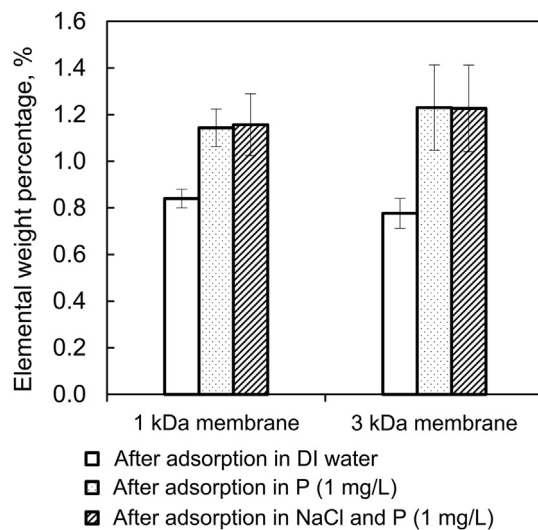


Fig. 2 – Weight percentage of P element on the ceramic membranes after adsorption in DI water, NaH_2PO_4 solution and $\text{NaH}_2\text{PO}_4 + \text{NaCl}$ solutions (explicated in [Table 2](#)). Results were derived from EDX measurements, examined at 10 kV accelerating voltage and 500× magnification. The scan area was approximately 0.6 mm × 0.6 mm and three random areas were measured on each sample. Weight percentage of all elements detected is shown in [Supplementary Data, Table S2](#). Error bars show the SD from duplicate measurements.

Both membranes exhibited more negative surface charge with the addition of only $1 \text{ mg L}^{-1} \text{ PO}_4\text{-P}$ in the electrolytes, as shown in Fig. 1. This was probably due to the specific adsorption of phosphate on the TiO_2 . The phosphorus weight percentage on the membrane increased significantly after the membrane was rinsed with the phosphate solution or NaCl solution containing phosphate (Fig. 2), which indicated specific phosphate adsorption on the membranes.

A similar observation of a negative surface charge induced by adsorption of negatively charged arsenate and phosphate was also reported by Pena et al. (2006) and Randon et al. (1995), respectively. Both groups of researchers attributed the phosphate (arsenate) adsorption to the formation of tridentate (bidentate) bonding with TiO_2 .

The difference in surface charge between the measurements with and without phosphate addition became less significant regardless of the adsorption of phosphate in basic pH ranges of 8–9 (Fig. 1). The same observations were reported in studies on both arsenic (Liu et al., 2008; Pena et al., 2006) and phosphate (Randon et al., 1995) adsorption to TiO_2 . This less significant difference in surface charge results from the instability of TiO_2 -phosphate bonding (Randon et al., 1995; Schafer et al., 1991). Explicitly, the phosphate groups can detach from the TiO_2 surface by hydrolysis effect when increasing the solute pH (Alberti et al., 2000).

3.2. Effect of pH on phosphate rejection

Phosphate rejection by the ceramic membranes was tested at pH levels ranging from 6 to 9.5 with $6.0 \text{ mmol L}^{-1} \text{ NaCl}$ background electrolyte; results are shown in Fig. 3. Increasing the solution pH from 6 to 8.5 dramatically increased the phosphate rejection from 35% to 75% by the 1 kDa membrane (from 40% to 86% with 3 kDa membrane). At pH 8.5, the maximum rejection was obtained by both the 1 kDa and 3 kDa ceramic membranes. It is clear that phosphate cannot be rejected by the tight UF membranes by merely steric rejection because the

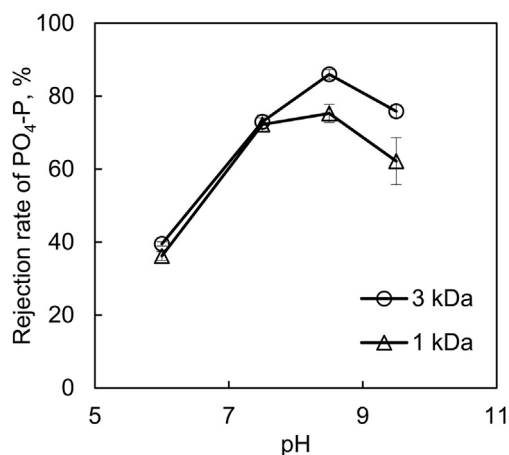


Fig. 3 – Effect of pH on phosphate rejection. The feed water contained $1.0 \text{ mg P L}^{-1} \text{ NaH}_2\text{PO}_4$, 6.0 mmol/l NaCl and NaOH of various concentrations to adjust corresponding pH values. The filtration conditions were as follows: cross-flow velocity 2.0 m s^{-1} and flux $50 \text{ L m}^{-2} \text{ h}^{-1}$. Error bars show the SD from duplicate experiments.

membranes' pore radii (1.77 nm and 3.06 nm for 1 and 3 kDa UF, respectively) are much larger than the hydrated size of H_2PO_4^- (0.102 nm) or HPO_4^{2-} (0.129 nm) (Araki et al., 1961).

However, the pH dependent rejection indicates the dominant role of electrostatic repulsion on the phosphate rejection by the tight UF membranes (Nghiem et al., 2005; Verliefde et al., 2007). Due to the charged groups on the internal pore walls, an excess of counter-ions accumulate at the pore surface, while the co-ions are partially excluded from this region (Donnan, 1924). Since the electrostatic repulsion increases as a function of the surface charge, the co-ions become more and more scattered in the double layer with an increasing charge, and thus have a more and more difficult task of entering the membrane pores. As a result, the rejection of the co-ions by electrostatic repulsion increases with an increase in the membrane's surface charge (Jamnik and Vlachy, 1995).

It is worthwhile to note that the 3 kDa membrane had a higher phosphate rejection than the 1 kDa membrane. If size exclusion were the main mechanism, the opposite trend should have been observed. In the current case, the higher rejection by the 3 kDa membrane can be attributed to the greater surface charge of this membrane and thus a stronger electrostatic repulsive force against the phosphate.

In addition, phosphate speciation changes from monovalent H_2PO_4^- to divalent HPO_4^{2-} when increasing the solution pH from 4 to 10. Thus, higher electrostatic repulsion from the negatively charged membrane occurs to divalent HPO_4^{2-} than on monovalent H_2PO_4^- . Moreover, the HPO_4^{2-} anion has a lower diffusion coefficient, $7.34 \times 10^{-10} \text{ m}^2 \text{ s}^{-1}$, than the H_2PO_4^- anion, $8.46 \times 10^{-10} \text{ m}^2 \text{ s}^{-1}$ (Table 3). These conditions can also contribute to the increased rejection with increasing pH (Brandhuber and Amy, 1998; Seidel et al., 2001). However, a slight decrease in rejection was observed when the pH increased from 8.5 to 9.5, as shown in Fig. 3. This was possibly because of the phosphate desorption from the membranes at pH above 9, as discussed in Section 3.1.

3.3. Effect of ionic strength and Debye ratio

As shown in Fig. 4 (left side), an increase in ionic strength from 0.5 to 6.0 mmol L^{-1} led to a slight decrease in the phosphate rejection, while further increasing the ionic strength to 20.0 mmol L^{-1} led to a significant decrease in the rejection. The increased ionic strength compresses the double layer on the membrane surface, which leads to a decreased Debye ratio (ratio of Debye length to membrane pore radius). A lower Debye ratio value means less double layer overlapping in the pores and the electrostatic interaction thus plays less of a role in ion rejection (Jacazio et al., 1972). A threshold Debye ratio can be defined as a Debye ratio under which a significant

Table 3 – Diffusion coefficients of anions at infinite dilution at 25 °C.

Anions	Diffusion coefficient, $\times 10^{-10} \text{ m}^2 \text{ s}^{-1}$
HPO_4^{2-}	7.34
H_2PO_4^-	8.46
SO_4^{2-}	10.65
Cl^-	20.32

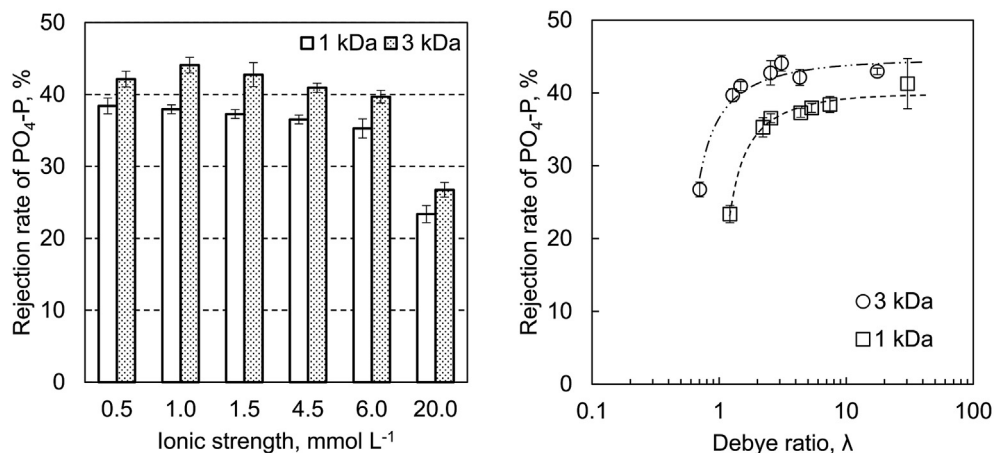


Fig. 4 – Effect of ionic strength (left side) and Debye ratios (right side) on phosphate rejection. The feed water contained $1.0 \text{ mg P L}^{-1} \text{ NaH}_2\text{PO}_4$ and NaCl of various concentrations ($0.5, 1.0, 1.5, 4.5, 6.0$ and 20.0 mmol L^{-1}). The pH was 6.0 ± 0.2 . The pore radii of 1 kDa and 3 kDa membranes were estimated with Eq. 4 as 0.69 nm and 1.14 nm , respectively. The filtration conditions were described in Fig. 3. Error bars show the SD from duplicate experiments.

decrease in rejection occurs. Various threshold Debye ratios, ranging from 0.6 to 2, were reported in other studies (Jacazio et al., 1972; Schaep et al., 1999). The Debye ratios of the tested conditions were plotted in Fig. 4 (right side). The threshold Debye ratios of 2 and 1 were observed on the 1 kDa and 3 kDa tight UF membranes, respectively. It appears that the threshold Debye ratio can vary with different membranes. This is due to differences in membrane characterization, e.g. pore size distribution and pore tortuosity. A broader pore size distribution will lead to a larger threshold Debye ratio than a membrane with narrower pore size distribution. An increased pore tortuosity enhances the salt rejection by the membrane (Musale and Kumar 2000), and may decrease the threshold Debye ratio. Therefore, the threshold Debye ratio should be determined for a specific membrane and solute.

It is clear that a Debye ratio higher than the threshold Debye ratio is an essential condition of electrostatic salt rejection by a tight UF or a loose nanofiltration membrane during water filtration. The wastewater treatment plant effluents in the Netherlands have ionic strengths between 5 and 20 mmol L^{-1} . Thus, under the conditions of high ionic strengths in effluent water treatment, a tighter membrane should be chosen in order to achieve electrostatic salt rejection.

3.4. Effect of divalent anions on the phosphate rejection

The effect of divalent anions on phosphate rejection was studied with two background solutions: NaCl and Na_2SO_4 . The two solutions have the same ionic strength to ensure both a constant Debye length in the membranes and a constant Debye ratio. The results show that divalent anion SO_4^{2-} decreases the phosphate rejection by about 10% on both 1 kDa and 3 kDa tight ceramic UF membranes (Fig. 5).

This is because the selective rejection of the anions by a negatively charged tight UF membrane can be influenced by both the Donnan effect and the diffusion. The Donnan effect

states that if the co-ion of a certain salt (i.e. the ion with a charge that is similar to the membrane charge) is rejected due to charge repulsion by the membrane, the counter-ion will also need to be rejected to maintain electroneutrality across the membrane and vice versa: the permeation of the counter-ion, due to convection, will draw the co-ions through the membrane due to unbalanced electroneutrality (Donnan, 1924). The diffusion due to concentration gradient is another driving force for the movement of ions during filtration with tight UF membrane. In addition, unlike an NF membrane, steric exclusion shows limited impact while diffusion of multivalent ions is relatively significant.

In a mixture of ions, the permeability of an individual ion can be governed by the diffusion coefficient and valence of each ion (Jacazio et al., 1972): the ions of higher diffusion coefficients and less charge are mostly subject to migration. The monovalent counter-ions Na^+ can easily move through the

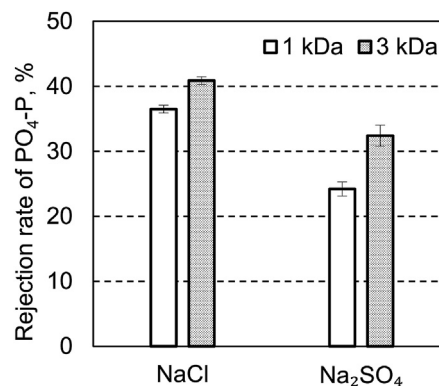


Fig. 5 – Rejection of phosphate under feed solution of A. $1.0 \text{ mg P L}^{-1} \text{ NaH}_2\text{PO}_4$ and $4.5 \text{ mmol L}^{-1} \text{ NaCl}$; B. $1.0 \text{ mg P L}^{-1} \text{ NaH}_2\text{PO}_4$ and $1.5 \text{ mmol L}^{-1} \text{ Na}_2\text{SO}_4$. The pH was 6.0 ± 0.2 . The filtration conditions were described in Fig. 3. Error bars show the SD from duplicate experiments.

membrane due to convection, diffusion and charge attraction from membrane surface. Meanwhile, the co-ions (phosphate, SO_4^{2-} and Cl^- in this case) tend to permeate through the tight UF membrane by the electroneutrality effect and concentration gradient. In the case of $\text{Cl}^-/\text{H}_2\text{PO}_4^-$ mixtures, the diffusion coefficient of Cl^- is much higher than H_2PO_4^- and thus more Cl^- anions permeate through the membrane. In the case of $\text{SO}_4^{2-}/\text{H}_2\text{PO}_4^-$ mixtures, SO_4^{2-} and H_2PO_4^- have similar diffusion coefficients (Table 3), while SO_4^{2-} ions bear more electrostatic repulsion from the membrane. Therefore, more H_2PO_4^- ions are dragged into the permeate solution by the electroneutrality effect and concentration gradient.

The competition for rejection between these ions is called co-ion competition (Luo and Wan, 2013). Similarly, studies by Szoke et al. (2003) and Déon et al. (2009) show that the Cl^- rejection in the mixture of NaCl and Na_2SO_4 solution is much less than that in an NaCl only solution by an NF with negative surface charge.

3.5. Effect of permeate flux and cross-flow rate

Table 4 shows that both the permeate flux and cross-flow rate substantially influence phosphate rejection. At the highest flux of $62 \text{ L m}^{-2} \text{ h}^{-1}$, a rejection of 47.5% was observed, and decreased permeate flux clearly led to lower rejection rates (38.4% at $25 \text{ L m}^{-2} \text{ h}^{-1}$). The flux-dependent rejection behaviour by tight UF membranes resembles that of common salt rejection membranes, such as NF and RO. The widely used solution-diffusion model assumes that both the solvent and the solute diffuse through the solute rejection layer of the membrane independently of each other under their respective chemical potential gradient. According to the solution-diffusion model, the water flux through the membrane is proportional to the net applied pressure, whereas the solute flux is proportional to the concentration difference across the solute rejection layer (Fane et al., 2011). As a result, the dilution effect takes place at a higher water flux.

Table 4 shows that the rejection increased as a function of the cross-flow rate and reached a plateau when the Reynolds number was equal to or higher than 2250 (transition to turbulent flow regime). It is suggested that concentration polarization occurred (Mulder, 1991). A study on concentration polarization phenomena by Déon et al. (2013) showed that the

thickness of the stagnant layer on the membrane decreases with increased cross-flow velocity, while the concentration gradient from the bulk to the membrane surface remains almost the same. An increased cross-flow (i.e. elevated turbulence) thus reduces the wall concentration when the bulk concentration remains unchanged. Consequently, the observed phosphate rejection rate increased as the Reynolds number of the cross-flow increased. Additionally, an increase from 1 m s^{-1} – 2 m s^{-1} in cross-flow rate increased the rejection rate by 1%. However, a higher cross-flow rate, in order to obtain a higher Reynolds number, leads to much higher energy consumption. It thus indicates a cross-flow of Reynolds number about 2250 as a cost-effective cross-flow regime.

3.6. Implication for RO pre-treatment and ceramic membrane development

To date, tubular ceramic membranes are less implemented at the industrial scale compared to polymeric membranes in spiral-wound or hollow fibre configurations, due to their relatively small active surface area and higher price per m^2 . However, results reported here have an important implication for the deployment of tight ceramic membranes in RO pre-treatment processes. The application of such membranes might be able to reach the minimum concentration of P, below $0.3 \mu\text{g P L}^{-1}$ (Vrouwenvelder et al., 2010), to avoid biofouling. Conventional coagulation can reduce the P concentration to 6 – $120 \mu\text{g L}^{-1}$ (Jacobson et al., 2009). Therefore, a P concentration that is lower than the P limitation might be achieved by coagulation coupled with a tight ceramic UF membrane. In addition, the combination of coagulation and the tight ceramic UF as RO pre-treatment may lead to a lower organic carbon concentration compared with conventional coagulation with UF. Because of the lower MWCO of tight UF compared to normal UF, a larger percentage of polysaccharides, proteins and natural organic matters, which are the main contributor to the organic fouling in RO (Ang et al., 2006, 2011), can be rejected by the tight UF and, thus, organic fouling in RO can be reduced.

In the experimental conditions, the rejection of phosphate is twofold higher under high pH conditions ($\text{pH} = 7.5$ – 9.5) than under neutral pH conditions (Fig. 6). This is because of the synergistic effect of speciation shifting and surface charge increase.

In practice, it should be noted that the interaction between organic matter and the membrane's surface (i.e. membrane fouling) will change the electrostatic interactions on phosphate rejection (Heijman et al., 2007; Xu et al., 2006). Studies show that NOM fouling and biofouling modify the zeta potential of the membrane surface to various values, ranging from -5 mV to -41 mV at $\text{pH} 6$ – 7 (Botton et al., 2012; Xie et al., 2013). Botton et al. (2012) reported that the biofouling on NF membranes does not affect the rejection of negatively charged pharmaceuticals. However, the effect of fouling by EfOM (effluent organic matter) and NOM on phosphate rejection has not been investigated.

In addition, characterizing selective ionic rejection with negatively charged tight UF and loose NF gives new insights for innovative processes on water treatment. For example, calcium phosphate scaling constrains the nanofiltration

Table 4 – Phosphate rejection by the 1 kDa membrane with various flux and cross-flow. The feed water contained 1.0 mg P L^{-1} NaH_2PO_4 dissolved with demi-water. The ionic strength and pH of the feed water were $0.032 \text{ mmol L}^{-1}$ and 6.0 ± 0.2 , respectively.

	Flux $\text{L m}^{-2} \text{ h}^{-1}$	Cross-flow velocity m s^{-1}	Reynolds number	Rejection ^a %
Effect	25		4490	38.4 ± 2.0
of	50	2.0	4490	41.3 ± 3.5
flux	62	2.0	4490	47.5 ± 0.8
Effect of	50	0.5	1120	31.4 ± 0.5
cross-	50	1.0	2250	40.2 ± 0.0
flow	50	2.0	4490	41.3 ± 3.5

^a Average \pm SD from duplicate measurements.

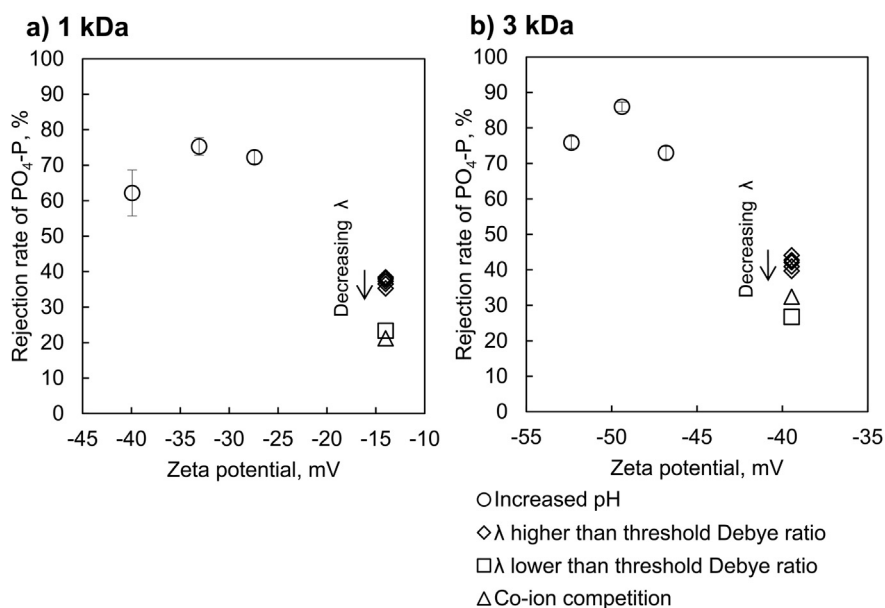


Fig. 6 – Impact of zeta potential, pH, Debye ratio (λ) and co-ion competition on the phosphate rejection by a) 1 kDa and b) 3 kDa ceramic membrane. Increasing pH leads to a significant increase in phosphate rejection due to increased surface charge and decreased permeate coefficient of HPO_4^{2-} rather than H_2PO_4^- . A decreasing Debye ratio does not considerably decrease the rejection until the Debye ratio falls lower than the threshold value. The SO_4^{2-} anion causes a significant decrease in rejection due to co-ion competition.

systems for water treatment and reuse (Heijman et al., 2003; Sperlich et al., 2010), whereas it does not likely occur in the negatively charged tight UF or loose NF system, because those systems are capable of rejecting phosphate but not able to remove calcium.

The results reported also suggest that development of ceramic tight UF or loose NF with negative surface charge will promote the application of ceramic membranes to water treatment and the wastewater reuse industry. On the one hand, ceramic material allows critical chemical cleaning without broadening the pore size distribution of the membrane. Broadened pore size distribution during chemical cleaning occurs in polymeric salt rejection membranes, which gradually disables their ability for salt rejection (Ballou and Wydeven, 1972). On the other hand, developing ceramic membranes with a tighter pore size and with a more negatively charged surface will promote the innovation of membrane processes on water treatment because it will lead to more effective rejection of the less diffusive anions, e.g. arsenate and phosphate.

4. Conclusions

In this paper, the phosphate rejection behaviour of 1 kDa and 3 kDa tight ceramic UF membranes was investigated and the feasibility of inducing phosphate limitations on RO by tight ceramic UF pre-treatment was discussed. The following conclusions can be drawn:

The negatively charged 1 kDa and 3 kDa tight ceramic UF membranes were capable of rejecting phosphate by electrostatic repulsion. Having Debye ratios above the typical

threshold Debye ratio was an essential condition to achieve salt rejection by the electrostatic repulsion mechanism. Under this condition, the phosphate rejection is governed by the membrane surface charge.

A more negatively charged 3 kDa membrane yielded a higher rejection rate than the 1 kDa membrane. Increased pH led to a dramatically increased rejection because the membranes were more negatively charged in the higher pH condition. The maximum phosphate rejection of 87% was achieved by the 3 kDa membrane at pH 8.5.

Higher permeate flux and higher cross-flow rates led to increased phosphate rejection due to less significant diffusion and concentration polarization. However, phosphate rejection decreased by approximately 10% in the Na_2SO_4 solution due to co-ion competition. In wastewater reuse installations, a combination of coagulation and negatively charged tight UF as an RO pre-treatment is recommended in order to limit biofouling in RO by inducing phosphate limitation.

Acknowledgements

This research project work was carried out in the framework of Agentschap NL-international InnoWATOR project “Innovative ceramic ultra and nanofiltration” and Shanghai Science and Technology Project for International Cooperation (Grant No. 12230707602). The authors acknowledge the PhD scholarship awarded to Ran Shang (No. 2009626042) by the China Scholarship Council. Dr. A.M.M. Al-Hadidi and K.W. Trzaskus at the University of Twente are acknowledged for the zeta potential measurements.

Appendix A. Supplementary data

Supplementary data related to this article can be found at <http://dx.doi.org/10.1016/j.watres.2013.10.008>.

REFERENCES

- Alami-Younssi, S., Larbot, A., Persin, M., Sarrazin, J., Cot, L., 1995. Rejection of mineral salts on a gamma alumina nanofiltration membrane application to environmental process. *J. Memb. Sci.* 102 (0), 123–129.
- Alberti, G., Marmottini, F., Cavalaglio, S., Severi, D., 2000. Intercalation processes of n-alkyl monoamines in γ -zirconium phosphate. *Langmuir* 16 (9), 4165–4170.
- Ang, W.S., Lee, S., Elimelech, M., 2006. Chemical and physical aspects of cleaning of organic-fouled reverse osmosis membranes. *J. Memb. Sci.* 272 (1–2), 198–210.
- Ang, W.S., Yip, N.Y., Tiraferri, A., Elimelech, M., 2011. Chemical cleaning of RO membranes fouled by wastewater effluent: achieving higher efficiency with dual-step cleaning. *J. Memb. Sci.* 382 (1–2), 100–106.
- Araki, T., Ito, M., Oscarsson, O., 1961. Anion permeability of the synaptic and non-synaptic motoneurone membrane. *J. Physiol.* 159 (3), 410–435.
- Ballou, E.V., Wydeven, T., 1972. Solute rejection by porous glass membranes. II. Pore size distributions and membrane permeabilities. *J. Colloid Interface Sci.* 41 (2), 198–207.
- Bandini, S., Vezzani, D., 2003. Nanofiltration modeling: the role of dielectric exclusion in membrane characterization. *Chem. Eng. Sci.* 58 (15), 3303–3326.
- Bartels, C.R., Wilf, M., Andes, K., Iong, J., 2005. Design considerations for wastewater treatment by reverse osmosis. *Water Sci. Technol.* 51, 473–482.
- Bellona, C., Drewes, J.E., 2005. The role of membrane surface charge and solute physico-chemical properties in the rejection of organic acids by NF membranes. *J. Memb. Sci.* 249 (1–2), 227–234.
- Boley, A., Narasimhan, K., Kieninger, M., Müller, W.R., 2010. Ceramic membrane ultrafiltration of natural surface water with ultrasound enhanced backwashing. *Water Sci. Technol.* 61 (5), 1121–1127.
- Botton, S., Verliefe, A.R., Quach, N.T., Cornelissen, E.R., 2012. Influence of biofouling on pharmaceuticals rejection in NF membrane filtration. *Water Res.* 46 (18), 5848–5860.
- Brandhuber, P., Amy, G., 1998. Alternative methods for membrane filtration of arsenic from drinking water. *Desalination* 117 (1–3), 1–10.
- Brandhuber, P., Amy, G., 2001. Arsenic removal by a charged ultrafiltration membrane-influences of membrane operating conditions and water quality on arsenic rejection. *Desalination* 140 (1), 1–14.
- Chevereau, E., Zouaoui, N., Limousy, L., Dutournié, P., Déon, S., Bourseau, P., 2010. Surface properties of ceramic ultrafiltration TiO₂ membranes: effects of surface equilibriums on salt retention. *Desalination* 255 (1–3), 1–8.
- Christoforou, C.C., Westermann-Clark, G.B., Anderson, J.L., 1985. The streaming potential and inadequacies of the Helmholtz equation. *J. Colloid Interface Sci.* 106 (1), 1–11.
- Déon, S., Dutournié, P., Fievet, P., Limousy, L., Bourseau, P., 2013. Concentration polarization phenomenon during the nanofiltration of multi-ionic solutions: Influence of the filtrated solution and operating conditions. *Water Res.* 47 (7), 2260–2272.
- Déon, S., Dutournié, P., Limousy, L., Bourseau, P., 2009. Transport of salt mixtures through nanofiltration membranes: numerical identification of electric and dielectric contributions. *Separation and Purification Technology* 69 (3), 225–233.
- Donnan, F.G., 1924. The theory of membrane equilibria. *Chem. Rev.* 1 (1), 73–90.
- Dubin, P.L., 1988. *Aqueous Size-exclusion Chromatography*. Elsevier.
- Fane, A.G., Tang, C.Y., Wang, R., 2011. In: Peter, W. (Ed.), *Treatise on Water Science*. Elsevier, Oxford, pp. 301–335.
- Ferry, J.D., 1936. Statistical evaluation of sieve constants in ultrafiltration. *J. General Physiol.* 20 (1), 95–104.
- Fievet, P., Sbaï, M., Szymczyk, A., 2005. Analysis of the pressure-induced potential arising across selective multilayer membranes. *J. Memb. Sci.* 264 (1–2), 1–12.
- Fievet, P., Sbaï, M., Szymczyk, A., Magnenet, C., Labbez, C., Vidonne, A., 2004. A new tangential streaming potential setup for the electrokinetic characterization of tubular membranes. *Sep. Sci. Technol.* 39 (13), 2931–2949.
- Fievet, P., Sbaï, M., Szymczyk, A., Vidonne, A., 2003. Determining the ζ -potential of plane membranes from tangential streaming potential measurements: effect of the membrane body conductance. *J. Memb. Sci.* 226 (1–2), 227–236.
- Greenberg, G., Hasson, D., Semiat, R., 2005. Limits of RO recovery imposed by calcium phosphate precipitation. *Desalination* 183 (1–3), 273–288.
- Gross, R.J., Osterle, J.F., 1968. Membrane transport characteristics of ultrafine capillaries. *J. Chem. Phys.* 49 (1), 228–234.
- Heijman, S.G.J., Folmer, H., Donker, F., Rietman, B.M., Schippers, J.C., 2003. Application of ScaleGuard® at reverse osmosis and nanofiltration installations. *Water Sci. Technol. Water Supply* 3 (5–6), 133–138.
- Heijman, S.G.J., Verliefe, A.R.D., Cornelissen, E.R., Amy, G., van Dijk, J.C., 2007. Influence of natural organic matter (NOM) fouling on the removal of pharmaceuticals by nanofiltration and activated carbon filtration. *Water Sci. Technol. Water Supply* 7 (4), 17–23.
- Herzberg, M., Berry, D., Raskin, L., 2010. Impact of microfiltration treatment of secondary wastewater effluent on biofouling of reverse osmosis membranes. *Water Res.* 44 (1), 167–176.
- Huisman, I.H., Trägårdh, G., Trägårdh, C., Pihlajamäki, A., 1998. Determining the zeta-potential of ceramic microfiltration membranes using the electroviscous effect. *J. Memb. Sci.* 147 (2), 187–194.
- Hunter, R.J., 1981. *Zeta Potential in Colloid Science: Principles and Applications*. Academic Press.
- Jacazio, G., Probst, R.F., Sonin, A.A., Yung, D., 1972. Electrokinetic salt rejection in hyperfiltration through porous materials. Theory and experiment. *J. Phys. Chem.* 76 (26), 4015–4023.
- Jacobson, J.D., Kennedy, M.D., Amy, G., Schippers, J.C., 2009. Phosphate limitation in reverse osmosis: an option to control biofouling? *Desali. Water Treat.* 5 (1–3), 198–206.
- Jamnik, B., Vlachy, V., 1995. Ion partitioning between charged micropores and bulk electrolyte solution. Mixtures of mono- and divalent counterions and monovalent co-ions. *J. Am. Chem. Soc.* 117 (30), 8010–8016.
- Kim, J., Davies, S.H.R., Baumann, M.J., Tarabara, V.V., Masten, S.J., 2008. Effect of ozone dosage and hydrodynamic conditions on the permeate flux in a hybrid ozonation-ceramic ultrafiltration system treating natural waters. *J. Memb. Sci.* 311 (1–2), 165–172.
- Kosmulski, M., 2003. A literature survey of the differences between the reported isoelectric points and their discussion. *Colloids Surf. A Physicochem. Eng. Aspects* 222 (1–3), 113–118.
- Labbez, C., Fievet, P., Thomas, F., Szymczyk, A., Vidonne, A., Foissy, A., Pagetti, P., 2003. Evaluation of the “DSPM” model on a titania membrane: measurements of charged and uncharged solute retention, electrokinetic charge, pore size,

- and water permeability. *J. Colloid Interface Sci.* 262 (1), 200–211.
- Larbot, A., Fabre, J.P., Guizard, C., Cot, L., 1988. Inorganic membranes obtained by sol-gel techniques. *J. Memb. Sci.* 39 (3), 203–212.
- Liu, G.J., Zhang, X.R., McWilliams, L., Talley, J.W., Neal, C.R., 2008. Influence of ionic strength, electrolyte type, and NOM on As(V) adsorption onto TiO₂. *J. Environ. Sci. Health Part A* 43 (4), 430–436.
- Luo, J., Wan, Y., 2013. Effects of pH and salt on nanofiltration – a critical review. *J. Memb. Sci.* 438 (0), 18–28.
- Luo, T., Cui, J., Hu, S., Huang, Y., Jing, C., 2010. Arsenic removal and recovery from copper smelting wastewater using TiO₂. *Environ. Sci. Technol.* 44 (23), 9094–9098.
- Miettinen, I.T., Vartiainen, T., Martikainen, P.J., 1997. Phosphorus and bacterial growth in drinking water. *Appl. Environ. Microbiol.* 63 (8), 3242–3245.
- Moritz, T., Benfer, S., Arki, P., Tomandl, G., 2001. Investigation of ceramic membrane materials by streaming potential measurements. *Colloids Surf. A Physicochem. Eng. Aspects* 195 (1–3), 25–33.
- Mulder, M. (Ed.), 1991. *Basic Principles of Membrane Technology*. Kluwer Academic Publishers.
- Musale, D.A., Kumar, A., 2000. Effects of surface crosslinking on sieving characteristics of chitosan/poly(acrylonitrile) composite nanofiltration membranes. *Sep. Purif. Technol.* 21 (1–2), 27–37.
- Nghiem, L.D., Schäfer, A.I., Elimelech, M., 2005. Pharmaceutical retention mechanisms by nanofiltration membranes. *Environ. Sci. Technol.* 39 (19), 7698–7705.
- Nghiem, L.D., Schäfer, A.I., Elimelech, M., 2006. Role of electrostatic interactions in the retention of pharmaceutically active contaminants by a loose nanofiltration membrane. *J. Memb. Sci.* 286 (1–2), 52–59.
- Parks, G.A., 1965. The isoelectric points of solid oxides, solid hydroxides, and aqueous hydroxo complex systems. *Chem. Rev.* 65 (2), 177–198.
- Pena, M., Meng, X., Korfiatis, G.P., Jing, C., 2006. Adsorption mechanism of arsenic on nanocrystalline titanium dioxide. *Environ. Sci. Technol.* 40 (4), 1257–1262.
- Petersson, I.U., Löberg, J.E.L., Fredriksson, A.S., Ahlberg, E.K., 2009. Semi-conducting properties of titanium dioxide surfaces on titanium implants. *Biomaterials* 30 (27), 4471–4479.
- Randon, J., Blanc, P., Paterson, R., 1995. Modification of ceramic membrane surfaces using phosphoric acid and alkyl phosphonic acids and its effects on ultrafiltration of BSA protein. *J. Memb. Sci.* 98 (1–2), 119–129.
- Sathasivan, A., Ohgaki, S., Yamamoto, K., Kamiko, N., 1997. Role of inorganic phosphorus in controlling regrowth in water distribution system. *Water Sci. Technol.* 35 (7), 37–44.
- Schaep, J., Vandecasteele, C., Peeters, B., Luyten, J., Dotremont, C., Roels, D., 1999. Characteristics and retention properties of a mesoporous γ -Al₂O₃ membrane for nanofiltration. *J. Memb. Sci.* 163 (2), 229–237.
- Schafer, W.A., Carr, P.W., Funkenbusch, E.F., Parson, K.A., 1991. Physical and chemical characterization of a porous phosphate-modified zirconia substrate. *J. Chromatogr. A* 587 (2), 137–147.
- Schneider, R.P., Ferreira, L.M., Binder, P., Bejarano, E.M., Góes, K.P., Slongo, E., Machado, C.R., Rosa, G.M.Z., 2005. Dynamics of organic carbon and of bacterial populations in a conventional pretreatment train of a reverse osmosis unit experiencing severe biofouling. *J. Memb. Sci.* 266 (1–2), 18–29.
- Seidel, A., Waypa, J.J., Elimelech, M., 2001. Role of charge (Donnan) exclusion in removal of arsenic from water by a negatively charged porous nanofiltration membrane. *Environ. Eng. Sci.* 18 (2), 105–113.
- Shang, R., van den Broek, W.B.P., Heijman, S.G.J., van Agtmaal, S., Rietveld, L.C., 2011. Wastewater reuse through RO: a case study of four RO plants producing industrial water. *Desal. Water Treat.* 34 (1–3), 408–415.
- Sperlich, A., Warschke, D., Wegmann, C., Ernst, M., Jekel, M., 2010. Treatment of membrane concentrates: phosphate removal and reduction of scaling potential. *Water Sci. Technol.* 61 (2), 301–306.
- Szoke, S., Patzay, G., Weiser, L., 2003. Characteristics of thin-film nanofiltration membranes at various pH-values. *Desalination* 151 (2), 123–129.
- Szymczyk, A., Fievet, P., 2005. Investigating transport properties of nanofiltration membranes by means of a steric, electric and dielectric exclusion model. *J. Memb. Sci.* 252 (1–2), 77–88.
- Tsuru, T., Hironaka, D., Yoshioka, T., Asaeda, M., 2001. Titania membranes for liquid phase separation: effect of surface charge on flux. *Sep. Purif. Technol.* 25 (1–3), 307–314.
- Van Agtmaal, J., de Boks, P.A., Cornips, R., Paping, L.L.M.J., 2007. Evaluation of Feed Water Sources and Retrofitting of an Integrated Membrane System. IWA, Antwerpen, pp. 1–8.
- Verliefde, A.R.D., Cornelissen, E.R., Heijman, S.G.J., Verberk, J.Q.J.C., Amy, G.L., Van Der Bruggen, B., Van Dijk, J.C., 2008. The role of electrostatic interactions on the rejection of organic solutes in aqueous solutions with nanofiltration. *J. Memb. Sci.* 322 (1), 52–66.
- Verliefde, A.R.D., Heijman, S.G.J., Cornelissen, E.R., Amy, G., Van der Bruggen, B., Van Dijk, J.C., 2007. Influence of electrostatic interactions on the rejection with NF and assessment of the removal efficiency during NF/GAC treatment of pharmaceutically active compounds in surface water. *Water Res.* 41 (15), 3227–3240.
- Vrouwenvelder, J.S., Beyer, F., Dahmani, K., Hasan, N., Galjaard, G., Kruithof, J.C., Van Loosdrecht, M.C.M., 2010. Phosphate limitation to control biofouling. *Water Res.* 44 (11), 3454–3466.
- Xie, M., Nghiem, L.D., Price, W.E., Elimelech, M., 2013. Impact of humic acid fouling on membrane performance and transport of pharmaceutically active compounds in forward osmosis. *Water Res.* 47 (13), 4567–4575.
- Xu, P., Drewes, J.E., Kim, T.-U., Bellona, C., Amy, G., 2006. Effect of membrane fouling on transport of organic contaminants in NF/RO membrane applications. *J. Memb. Sci.* 279 (1–2), 165–175.
- Yaroshchuk, A., Ribitsch, V., 2002. Role of channel wall conductance in the determination of ζ -potential from electrokinetic measurements. *Langmuir* 18 (6), 2036–2038.
- Yaroshchuk, A.E., 2000. Dielectric exclusion of ions from membranes. *Adv. Colloid Interface Sci.* 85 (2–3), 193–230.

List of abbreviations

- EDX: Energy dispersive x-ray
 EfOM: Effluent organic matter
 IEP: Isoelectric point
 IS: Ionic strength
 RO: Reverse osmosis
 MWCO: Molecular weight cut-off
 UF: Ultrafiltration